Canadian Science Publishing | Transactions of the Canadian Society for Mechanical Engineering

Tracking Control of an Underwater Manipulator Using Fractional Integral Sliding Mode and Disturbance Observer

Journal:	*Transactions of the Canadian Society for Mechanical Engineering*
Manuscript ID	TCSME-2019-0225.R1
Manuscript Type:	Article
Date Submitted by the Author:	27-Dec-2019
Complete List of Authors:	Han, Lijun; Huazhong University of Science and Technology, school of naval architecture and ocean engineering Tang, Guoyuan; Huazhong University of Science and Technology, school of naval architecture and ocean engineering Xu, Ruikun; Huazhong University of Science and Technology, school of naval architecture and ocean engineering Huang, Hui; Huazhong University of Science and Technology, school of naval architecture and ocean engineering Xie, De; Huazhong University of Science and Technology, school of naval architecture and ocean engineering
Keywords:	fractional integral sliding mode control, disturbance observer, finite-time stability, trajectory tracking, underwater manipulator
Is the invited manuscript for consideration in a Special Issue? :	Not applicable (regular submission)

Tracking Control of an Underwater Manipulator Using Fractional Integral Sliding Mode and Disturbance Observer

The first author: Lijun Han,

Affiliation:

1.School of Naval Architecture and Ocean Engineering, Huazhong University of Science and Technology, Wuhan, China

Corresponding author: Guoyuan Tang,

E-mail: tgyuan@hust.edu.cn

Affiliation:

1.School of Naval Architecture and Ocean Engineering, Huazhong University of Science and Technology, Wuhan, China

Co-author: Ruikun Xu,

Affiliation:

1.School of Naval Architecture and Ocean Engineering, Huazhong University of Science and Technology, Wuhan, China

Co-author: Hui Huang,

Affiliation:

1.School of Naval Architecture and Ocean Engineering, Huazhong University of Science and Technology, Wuhan, China

Co-author: De Xie,

Affiliation:

1.School of Naval Architecture and Ocean Engineering, Huazhong University of Science and Technology, Wuhan, China

Abstract

In this paper, a fractional integral sliding mode control (FISMC) strategy with a disturbance observer (DO) is proposed for the trajectory tracking problem of the underwater manipulator, under lumped disturbances namely parameter uncertainties and external disturbances. The modified fractional integral sliding mode surface (FISMS) is designed to guarantee the fast convergence of system states. The DO method and the second-order sliding mode control law are used in the controller design, in which the former is introduced to compensate the effect of the lumped disturbances. Also, a saturated function is selected to replace the sign function to attenuate the chattering phenomenon. The stability of the overall closed-loop system is proved via Lyapunov's finite-time stability theory. Numerical simulations are performed on a 6 degree of freedom (DOF) underwater manipulator. Simulation results demonstrate that the proposed control scheme can achieve better tracking performance and stronger robustness against disturbances, by comparing with the DO-based PD control and the DO-based PID-type linear sliding mode control (SMC).

Keywords: fractional integral sliding mode control; disturbance observer; finite-time stability; trajectory tracking; underwater manipulator

1. Introduction

Unmanned underwater vehicles (UUVs) equipped with one or more underwater manipulators, play an indispensable role in the fields of marine scientific research and resource exploration and development (e.g., Antonelli 2006; Sivcev et al. 2018). Since these manipulators have uncertainties due to high coupling and time-varying nonlinearity, and are affected by the external disturbances like payload variations, underwater currents, etc., it is more difficult to control than those operated in air. Some advanced control methods (e.g., Wit et al. 2000; Lee and Choi 2000; Pandian and Sakagami 2010; Patompak and Nilkhamhang 2012) have been proposed to overcome these issues. Wit et al. (2000) has proposed a control method based on singular perturbation theory for an UVMS with disturbances; Lee and Choi (2000) presented a robust control based on neural network and backpropagation learning algorithm for an underwater manipulator with uncertainties, in which the neural network gains were determined by trial and error; Pandian and Sakagami (2010) proposed a neurol-fuzzy control approach with feedback gain adjustment and dynamic estimate for multi-link underwater manipulator depending on neural networks with more training data; Patompak and Nilkhamhang (2012) delivered an adaptive SMC based on the backstepping method for underwater robotic vehicles with parametric uncertainties and external disturbances. The above methods can make the system have a good tracking performance, but they have only discussed their asymptotically stable property. This paper devotes to designing an appropriate controller to achieve faster convergence and better robustness for underwater manipulators with the lumped disturbances, including dynamics uncertainties and external disturbances.

Generally, SMC has quite good natures such as fast convergence and insensitive to uncertainties, where sliding mode surface is taken as a key factor (Feng et al. 2014). The conventional linear sliding mode surfaces like PD-type (Xu et al. 2007) can only make the system errors achieve the asymptotic convergence to equilibrium, while the nonlinear ones can ensure the finite-time convergence, e.g., terminal sliding mode control (TSMC) (Mobayen 2015). And, the method in Xu et al. (2007) can guarantee the asymptotic stability of the system, but in lack of discussing its finite-time stability. Mobayen (2015) has proposed a TSMC scheme that can make the system achieve the finite-time stability, but the singularity problem still exists in it. To handle such issue, some nonsingular TSMC methods (e.g., Liu and Zhang 2013; Wang et al. 2016, 2019a, 2019b, 2019c) have been proposed for the controller design, in which different ways are required for modifying the sliding mode surfaces. Among, fractional-order nonsingular terminal sliding mode control (FONTSMC) strategies (e.g. Wang et al. 2016, 2019b, 2019c) have been reported according to the fractional-order integrator and differentiator theory. They can all take advantage of the extra fractional-order DOF compared to only integer-order TSMC (e.g., Liu and Zhang 2013; Wang et al. 2019a). Moreover, another control method in Basin et al. (2016) has been proposed for the finite-time convergence being expanded to the fixed-time convergence, in which it can obtain the uniform bounded settling time and not involve in the initial system states. The improvement can be a quite difference from the above-mentioned FONTSMC strategies. Combining this advantage and the singularity-free requirement, in this paper a modified FISMC method is proposed which can achieve the finite-time convergence and also avoid the singular problem.

Another problem is to deal with the dynamics uncertainties and external disturbances of the underwater manipulator. For such situation, an adaptive SMC scheme in Liang and Li (2014) has been adopted for the attitude tracking problem, where the adaptive technique was utilized to estimate the upper bounds of the lumped disturbances including system uncertainties and external disturbances. Based on a distributed fast TSMC strategy, Hussian et al. (2017) has used the assumed known function to handle the bounded uncertainties of the system. Compared with the researches (e.g., Liang and Li 2014; Hussian et al. 2017), Dinh et al. (2018) has proposed a robust controller for the electro-hydraulic manipulator in which a DO was presented to estimate the bounded lumped disturbances. To estimate the bounds of such states, Huang et al. (2019) and (2020) have addressed the interval observer design problems of both discrete-time and asynchronous switched systems, respectively. Since only a few literatures considered the convergence of the estimation errors for the uncertainties or external disturbances, in this paper another DO (e.g., Shtessel et al. 2007) was introduced to handle this problem. The exploitation of such DO method was to guarantee that the estimation errors can converge to zero in finite time. In other words, after a certain finite time the control system can still be stable, and would not be affected by disturbances.

Motivated by aforementioned analyses, a FISMC scheme with a DO is proposed to solve the trajectory tracking problem of the base-fixed underwater manipulator, which is subjected to the lumped disturbances including dynamic uncertainties and the external disturbances. The primary objective of this scheme is to make the system realize the finite-time stability, and to ensure the finite-time convergence of the estimation errors of the lumped disturbances. Since the proposed controller refers to the design of the modified FISMS, the state error of the system can achieve the finite-time convergence

without the appearance of singular conditions in the derivation process. The DO method is utilized to alleviate the effect of the lumped disturbances so as to achieve the finite-time convergence of the estimation errors. On this basis, the second-order sliding mode control law is introduced in the design of the system controller. Furthermore, this paper adopts a saturated function to replace the sign function in order to deal with the chattering issue. Through the finite-time stability theory, the overall system can achieve the finite-time stability, which guarantees its fast convergence, high-precision tracking performance and good robustness against disturbances. Simulation results demonstrate the effectiveness of the proposed controller in comparison with other control schemes.

To conclude, the contributions in this paper are concisely described in the following. (1) To propose a modified FISMS. It can make the state errors realize the finite-time convergence and avoid the singularity problem. (2) To design a modified FISMC scheme with a DO. Base on the modified FISMS, combing the DO method and second-order sliding mode control law, the proposed method can guarantee the finite-time stability of the system and the finite-time convergence of the disturbance estimation errors. (3) To testify the validation of the proposed control through the comparative simulation results.

This paper is organized as follows. Firstly, section II presents the tracking purpose of the underwater manipulator along with its dynamic analysis. Section III describes a FISMC algorithm with a DO and analyses the finite-time stability of the system. In section IV, numerical simulations are performed on a 6 DOF underwater manipulator. Finally, several conclusions are drawn in section V.

2. Problem description

This paper primarily considers the control problem that a fixed-base underwater manipulator tracks a small underwater vehicle in the short-range phase, meanwhile, the

target trajectory is assumed within the workspace of the manipulator end effector. Here, a 6 DOF underwater manipulator is selected, and its configuration is shown in Fig. 1. In addition, its coordinate system is built by D-H notation (Craig 2004), which contains the base frame $o_0 - x_0 y_0 z_0$ and link frame $o_i - x_i y_i z_i (i = 1, \cdots, 6)$. For each link frame, four quantities are defined, including joint variable θ_i, link twist α_{i-1}, link length a_{i-1} and link offset d_i $(i = 1, \cdots, 6)$.These link parameters are listed in Table 1.

2.1. The dynamics of the underwater manipulator

In the following, the dynamics of an underwater manipulator with m DOF instead of only 6 DOF would be presented. Based on the Lagrange function and the strip theory (Dunnigan and Russell 1998), its dynamic equation with hydrodynamic effects is established and expressed in the form:

$$\mathbf{M}(\boldsymbol{\theta})\ddot{\boldsymbol{\theta}} + \mathbf{C}(\boldsymbol{\theta}, \dot{\boldsymbol{\theta}})\dot{\boldsymbol{\theta}} + \boldsymbol{G}(\boldsymbol{\theta}) + \boldsymbol{B}(\boldsymbol{\theta}) + \boldsymbol{\tau}_h + \boldsymbol{\tau}_d = \boldsymbol{\tau} \tag{1}$$

where $\boldsymbol{\theta}$, $\dot{\boldsymbol{\theta}}$, $\ddot{\boldsymbol{\theta}} \in \boldsymbol{R}^m$ stand for the joint position vector, joint velocity vector, and joint acceleration vector, respectively. $\mathbf{M}(\boldsymbol{\theta}) \in \mathbf{R}^{m \times m}$ is defined as the symmetric and positive definite inertial matrix and $\mathbf{C}(\boldsymbol{\theta}, \dot{\boldsymbol{\theta}}) \in \mathbf{R}^{m \times m}$ is the Coriolis and centrifugal matrix. $\boldsymbol{G}(\boldsymbol{\theta})$, $\boldsymbol{B}(\boldsymbol{\theta}) \in \boldsymbol{R}^m$ are the gravitational and buoyancy vectors. $\boldsymbol{\tau}_h \in \boldsymbol{R}^m$ represents the hydrodynamic torque vector caused by fluid acceleration force, water resistance and additional mass force. $\boldsymbol{\tau}_d \in \boldsymbol{R}^m$ denotes the external disturbance like payload variations and underwater currents, and $\boldsymbol{\tau} \in \boldsymbol{R}^m$ is the joint input torque. Then, the dynamic eq. (1) can be rewritten as

$$\mathbf{M}_0(\boldsymbol{\theta})\ddot{\boldsymbol{\theta}} + \boldsymbol{H}_0(\boldsymbol{\theta}, \dot{\boldsymbol{\theta}}) + \Delta \boldsymbol{H}(\boldsymbol{\theta}, \dot{\boldsymbol{\theta}}) + \boldsymbol{\tau}_d = \boldsymbol{\tau} \tag{2}$$

where $\Delta\mathbf{M}(\boldsymbol{\theta}) = \mathbf{M}(\boldsymbol{\theta}) - \mathbf{M}_0(\boldsymbol{\theta})$, $\Delta\boldsymbol{H}(\boldsymbol{\theta},\dot{\boldsymbol{\theta}}) = \Delta\mathbf{M}(\boldsymbol{\theta})\ddot{\boldsymbol{\theta}} + \Delta\mathbf{C}(\boldsymbol{\theta},\dot{\boldsymbol{\theta}})\dot{\boldsymbol{\theta}} + \Delta\boldsymbol{G}(\boldsymbol{\theta}) + \Delta\boldsymbol{B}(\boldsymbol{\theta}) + \Delta\boldsymbol{\tau}_h$, $\boldsymbol{H}_0(\boldsymbol{\theta},\dot{\boldsymbol{\theta}}) = \mathbf{C}_0(\boldsymbol{\theta},\dot{\boldsymbol{\theta}})\dot{\boldsymbol{\theta}} + \boldsymbol{G}_0(\boldsymbol{\theta}) + \boldsymbol{B}_0(\boldsymbol{\theta}) + \boldsymbol{\tau}_{h0}$. Among them, $\mathbf{M}_0(\boldsymbol{\theta})$, $\mathbf{C}_0(\boldsymbol{\theta},\dot{\boldsymbol{\theta}})$, $\boldsymbol{G}_0(\boldsymbol{\theta})$, $\boldsymbol{B}_0(\boldsymbol{\theta})$, $\boldsymbol{\tau}_{h0}$ are known nominal values of the model parameter variables, and $\Delta\mathbf{M}(\boldsymbol{\theta})$, $\Delta\mathbf{C}(\boldsymbol{\theta},\dot{\boldsymbol{\theta}})$, $\Delta\boldsymbol{G}(\boldsymbol{\theta})$, $\Delta\boldsymbol{B}(\boldsymbol{\theta})$, $\Delta\boldsymbol{\tau}_h$ are uncertain model parameters.

A new variable $\boldsymbol{x} = [\boldsymbol{x}_1^{\mathrm{T}}, \boldsymbol{x}_2^{\mathrm{T}}]^{\mathrm{T}}$ is introduced into eq. (2), satisfying $\boldsymbol{x}_1 = \boldsymbol{\theta}$ and $\boldsymbol{x}_2 = \dot{\boldsymbol{\theta}}$, so eq. (2) can be described as follows,

$$\begin{cases} \dot{\boldsymbol{x}}_1 = \boldsymbol{x}_2 \\ \dot{\boldsymbol{x}}_2 = \mathbf{M}_0^{-1}(\boldsymbol{x}_1)(-\boldsymbol{H}_0(\boldsymbol{x}) + \boldsymbol{\tau}) + \boldsymbol{d} \end{cases} \tag{3}$$

where $\boldsymbol{d} = -\mathbf{M}_0^{-1}(\boldsymbol{x}_1)\Delta\boldsymbol{H}(\boldsymbol{x}) + \boldsymbol{d}_\tau$, $\boldsymbol{d}_\tau = -\mathbf{M}_0^{-1}(\boldsymbol{x}_1)\boldsymbol{\tau}_d$, and $\boldsymbol{d}$ denotes the lumped disturbance vector of the dynamic system, namely parameter uncertainties and external disturbances.

2.2. Preliminaries

In the paper, some notations are defined:

$\|\boldsymbol{\varphi}\|_1 = \sum_{i=1}^{n} |\varphi_i|$, $\|\boldsymbol{\varphi}\|_2 = \sqrt{\boldsymbol{\varphi}^{\mathrm{T}}\boldsymbol{\varphi}}$, $[\varphi_1^{\alpha_1}] = sign(\varphi_1)|\varphi_1|^{\alpha_1}$, $[\boldsymbol{\varphi}^{\boldsymbol{\alpha}}] = [[\varphi_1^{\alpha_1}], \cdots, [\varphi_n^{\alpha_n}]]^{\mathrm{T}}$, $[\boldsymbol{\varphi}^r] = [[\varphi_1^r], \cdots, [\varphi_n^r]]^{\mathrm{T}}$, where $r \in R_+$, $\boldsymbol{\varphi} = [\varphi_1, \cdots, \varphi_n]^{\mathrm{T}} \in \boldsymbol{R}^n$, $\boldsymbol{\alpha} = [\alpha_1, \cdots, \alpha_n]^{\mathrm{T}} \in \boldsymbol{R}_+^n$.

Assumption 1: The lumped disturbance vector $\boldsymbol{d}$ is twice differentiable, and there exists a known positive constant L_d satisfying $\|\ddot{\boldsymbol{d}}\|_1 \le L_d$.

Lemma 1 (Basin et al. 2016) : Consider the system $\dot{y}_1 = y_2, \cdots, \dot{y}_{n-1} = y_n, \dot{y}_n = u$, if the control input is assigned as $u = u_1(t) + u_2(t)$, satsfying $u_1(t) = -\beta_1[y_1^{\eta_1}] - \cdots - \beta_n[y_n^{\eta_n}]$ and $u_2(t) = -\kappa_1[y_1^{\varpi_1}] - \cdots - \kappa_n[y_n^{\varpi_n}]$, where $\beta_1, \cdots, \beta_n > 0$, $\kappa_1, \cdots, \kappa_n > 0$ are selected such that the polynomials $\phi^n + \beta_n\phi^{n-1} + \cdots + \beta_2\phi + \beta_1$ and $\phi^n + \kappa_n\phi^{n-1} + \cdots + \kappa_2\phi + \kappa_1$ are all Hurwitz; $\eta_1, \cdots, \eta_n$ satisfy $\eta_{i-1} = \eta_i\eta_{i+1}/(2\eta_{i+1} - \eta_i)$ with $\eta_{n+1} = 1$ and $\eta_n = \eta$; $\varpi_1, \cdots, \varpi_n$

satisfy $\varpi_{i-1} = \varpi_i \varpi_{i+1} / (2\varpi_{i+1} - \varpi_i)$ with $\varpi_{n+1} = 1$ and $\varpi_n = \varpi$, thus there exists small $\vartheta_1, \vartheta_2 \in (0,1)$ such that, for every $\eta \in (1-\vartheta_1, 1)$, $\varpi \in (1, 1+\vartheta_2)$, the system state defined as $\boldsymbol{y} = [y_1, y_2, \cdots, y_n]^{\mathrm{T}} \in \boldsymbol{R}^n$ can converge to the origin within a fixed time which does not depend on the initial condition.

3. The design of controller

The desired joint position vector $\boldsymbol{\theta}_d$ is assumed to be twice differentiable, and define its joint position error $\boldsymbol{\theta}_e$ and joint velocity error $\boldsymbol{\omega}_e$, i.e. $\boldsymbol{\theta}_e = \boldsymbol{\theta} - \boldsymbol{\theta}_d$ and $\boldsymbol{\omega}_e = \dot{\boldsymbol{\theta}} - \dot{\boldsymbol{\theta}}_d$. The control objective is that joint position vector $\boldsymbol{\theta}$ can track the desired $\boldsymbol{\theta}_d$ in finite time.

The FISM variable $\boldsymbol{s}$ is defined as follows,

$$\boldsymbol{s} = \boldsymbol{\omega}_e + \mathbf{C}_2 \int_0^t ([\boldsymbol{\omega}_e^{\boldsymbol{\alpha}_2}] + [\boldsymbol{\omega}_e^{\boldsymbol{\varpi}_2}])dt + \mathbf{C}_1 \int_0^t ([\boldsymbol{\theta}_e^{\boldsymbol{\alpha}_1}] + [\boldsymbol{\theta}_e^{\boldsymbol{\varpi}_1}])dt \tag{4}$$

where $\boldsymbol{s} = [s_1, \cdots, s_m]^{\mathrm{T}}$ and $\mathbf{C}_h = \mathrm{diag}[c_{h1}, \cdots, c_{hm}]$, $\boldsymbol{\alpha}_h = [\alpha_{h1}, \cdots, \alpha_{hm}]^{\mathrm{T}}$, $\boldsymbol{\varpi}_h = [\varpi_{h1}, \cdots, \varpi_{hm}]^{\mathrm{T}}$, $h = 1, 2$. Besides, their constant components c_{1i}, c_{2i}, α_{1i}, α_{2i}, ϖ_{1i}, ϖ_{2i} are selected referring to Lemma 1, satisfying c_{1i}, $c_{2i} > 0$, $0 < \alpha_{2i} < 1$, $\alpha_{1i} = \alpha_{2i} / (2 - \alpha_{2i})$, and $1 < \varpi_{2i} < 2$, $\varpi_{1i} = \varpi_{2i} / (2 - \varpi_{2i})$ $(i = 1, \cdots, m)$. This modified sliding mode surface can relax the requirement for the initial states and finally make the system states achieve the finite-time convergence. Meanwhile, the integral technique is used to avoid the singular conditions in the derivation process. Detailed explanations are shown in eq. (5).

In the sliding phase $s_i(t) = 0$, $i = 1, \cdots, m$, and its derivation meets $\dot{s}_i(t) = 0$, namely

$$\dot{\omega}_{ei} + c_{2i}([\omega_{ei}^{\alpha_{2i}}] + [\omega_{ei}^{\varpi_{2i}}]) + c_{1i}([\theta_{ei}^{\alpha_{1i}}]) + [\theta_{ei}^{\varpi_{1i}}]) = 0 \tag{5}$$

From the case of $n=2$ in Lemma 1, eq. (5) can be transformed into the similar situation: consider the control system $\dot{\theta}_{ei}=\omega_{ei}, \dot{\omega}_{ei}=u$, with $[\theta_{ei},\omega_{ei}]^{\mathrm{T}} \in \boldsymbol{R}^2$ being defined as its state. If the control input is chosen as $u=-c_{2i}([\omega_{ei}^{\alpha_{2i}}]+[\omega_{ei}^{\varpi_{2i}}])-c_{1i}([\theta_{ei}^{\alpha_{1i}}])+[\theta_{ei}^{\varpi_{1i}}])$, by use of the Lemma 1, thus there exists small $\vartheta_1,\vartheta_2 \in (0,1)$ such that, for every $\alpha_{2i} \in (1-\vartheta_1,1)$, $\varpi_{2i} \in (1,1+\vartheta_2)$, the system state $[\theta_{ei},\omega_{ei}]^{\mathrm{T}}$ can converge to the origin within a fixed time which does not depend on the initial condition. Similarly considering $i=1,\cdots,m$, it can be concluded that in any initial conditions the joint position error $\boldsymbol{\theta}_e$ can converge to the origin in finite-time.

In view of the eq. (3), the error dynamic equation can be expressed as follows,

$$\dot{\boldsymbol{\omega}}_e = \boldsymbol{F}_\omega + \boldsymbol{U}_\omega + \boldsymbol{d} \tag{6}$$

where $\boldsymbol{F}_\omega = -\mathbf{M}_0^{-1}(\boldsymbol{x}_1)\boldsymbol{H}_0(\boldsymbol{x}) - \ddot{\boldsymbol{\theta}}_d$ and $\boldsymbol{U}_\omega = \mathbf{M}_0^{-1}(\boldsymbol{x}_1)\boldsymbol{\tau}$. For convenience, the scalar formulations of the equation in eq. (6) are presented, namely

$$\dot{\omega}_{ei} = F_{\omega i} + U_{\omega i} + d_i, i=1,\cdots,m \tag{7}$$

Then, referring to Shtessel et al. (2007), the finite-time DO is introduced to estimate the lumped disturbance vector $\boldsymbol{d}$,

$$\begin{aligned}
&\dot{z}_0^i = v_0^i + F_{\omega i} + U_{\omega i},\ v_0^i = -\lambda_0 L^{1/3}[(z_0^i-\omega_{ei})^{2/3}] + z_1^i \\
&\dot{z}_1^i = v_1^i,\ v_1^i = -\lambda_1 L^{1/2}[(z_1^i - v_0^i)^{1/2}] + z_2^i \\
&\dot{z}_2^i = -\lambda_2 L\, sign(z_2^i - v_1^i) \\
&\hat{\omega}_{ei} = z_0^i, \hat{d}_i = z_1^i, \dot{\hat{d}}_i = z_2^i, i=1,\cdots,m
\end{aligned} \tag{8}$$

where L is a positive constant satisfying $|\ddot{d}_i| \le L$ $(i=1,\cdots,m)$ and $\lambda_j > 0 (j=1,2,3)$ are the observer coefficients. And the variables $\hat{\omega}_{ei}, \hat{d}_i, \dot{\hat{d}}_i$ denote the estimation of z_0^i, z_1^i, z_2^i, respectively. Define their estimation errors $e_0^i = z_0^i - \omega_{ei}$, $e_1^i = z_1^i - d_i$, $e_2^i = z_2^i - \dot{d}_i$,

$i = 1, \cdots, m$. Combining eqs. (7) and (8), the dynamic equations of the estimation errors are transformed into

$$\begin{aligned} \dot{e}_0^i &= -\lambda_0 L^{1/3}[(e_0^i)^{2/3}] + e_1^i \\ \dot{e}_1^i &= -\lambda_1 L^{1/2}[(e_1^i - \dot{e}_0^i)^{1/2}] + e_2^i \\ \dot{e}_2^i &= -\lambda_2 L\, sign(e_2^i - \dot{e}_1^i) - \ddot{d}_i \end{aligned} \tag{9}$$

From the analysis in Shtessel et al. (2007), it can be concluded that in eq. (9) the estimation errors are bounded, and meanwhile there exist a finite time T_1 such that the estimation errors can converge to zeros. Then the control scheme can be obtained based on the following Theorem 1.

Theorem 1: For the dynamic system in eq. (6), the finite-time stability of the system can be achieved via the following second-order sliding-mode control law:

$$\begin{aligned} \boldsymbol{U}_\omega &= -\mathbf{C}_2([\boldsymbol{\omega}_e^{\boldsymbol{\alpha}_2}] + [\boldsymbol{\omega}_e^{\boldsymbol{\varpi}_2}]) - \mathbf{C}_1([\boldsymbol{\theta}_e^{\boldsymbol{\alpha}_1}] + [\boldsymbol{\theta}_e^{\boldsymbol{\varpi}_1}]) - \hat{\boldsymbol{d}} - \boldsymbol{F}_\omega - \mathbf{K}_p[\boldsymbol{s}^{2/3}] + \boldsymbol{w}_n \\ \dot{\boldsymbol{w}} &= -\mathbf{K}_w[\boldsymbol{s}^{1/3}] \end{aligned} \tag{10}$$

where control gains $\mathbf{K}_p = \mathrm{diag}[k_{p1}, \cdots, k_{pm}]$, $\mathbf{K}_w = \mathrm{diag}[k_{w1}, \cdots, k_{wm}]$ and their components are all positive constants. Here define $\boldsymbol{w} = [w_1, \cdots, w_m]^{\mathrm{T}}$ as an auxiliary term.

Proof: Choose the positive definite Lyapunov function candidate as follows to analyze the system stability:

$$V_1 = \sum_{i=1}^{m} w_i^2 + \sum_{i=1}^{m} \int_0^{s_i} k_{wi}[v^{1/3}]dv \tag{11}$$

In view of eqs. (4) and (10), the dynamic equation in eq. (6) turns to be

$$\begin{aligned} \dot{s}_i &= -e_1^i - k_{pi}[s_i^{2/3}] + w_i, i = 1, \cdots, m \\ \dot{w}_i &= -k_{wi}[s_i^{1/3}], i = 1, \cdots, m \end{aligned} \tag{12}$$

By utilizing eqs. (10) and (12), the time derivative of eq. (11) can be calculated as

$$\begin{aligned}\dot{V}_1 &= \sum_{i=1}^{m} w_i \dot{w}_i + \sum_{i=1}^{m} k_{wi}[s_i^{1/3}]\dot{s}_i \\ &= \sum_{i=1}^{m} (-w_i k_{wi}[s_i^{1/3}] + k_{wi}[s_i^{1/3}](-e_1^i - k_{pi}[s_i^{2/3}] + w_i)) \\ &= \sum_{i=1}^{m} (-k_{wi} e_1^i [s_i^{1/3}] - k_{wi} k_{pi} | s_i |)\end{aligned} \tag{13}$$

In eq. (13), it can be seen that $\dot{V}_1 \le \sum_{i=1}^{m} k_{wi} | e_1^i |$ if $| s_i | \le 1$ and $\dot{V}_1 \le \sum_{i=1}^{m} k_{wi} | e_1^i | | s_i |^{1/3} \le \sum_{i=1}^{m} k_{wi} | e_1^i | | s_i |^{4/3} \le \max_{i=1,\cdots,m} | e_1^i | V_1$ if $| s_i | > 1$. Since the estimation error e_1^i is always bounded, it can result from eq. (13) that V_1 and s_i will be bounded in finite time $[0, T_1]$. In addition, the estimation error remains $e_1^i = 0$ for $t \ge T_1$. In this case, the derivative of the Lyapunov function $\dot{V}_1 \le -\sum_{i=1}^{m} k_{wi} k_{pi} | s_i | \le 0$. Then, the dynamic equations in eq. (12) become

$$\begin{aligned}\dot{s}_i &= -k_{pi}[s_i^{2/3}] + w_i, i = 1, \cdots, m \\ \dot{w}_i &= -k_{wi}[s_i^{1/3}], i = 1, \cdots, m\end{aligned} \tag{14}$$

For this case, the derivative of the Lyapunov function $\dot{V}_1 \le -\sum_{i=1}^{m} k_{wi} k_{pi} | s_i | \le 0$. Therefore, s_i and w_i can achieve the asymptotic convergence to zero. According to Shtessel et al. (2007), the asymptotical stability implies the finite-time stability, namely, s_i can converge to zero in finite time. From the above analyses of eq. (5), the joint position error $\boldsymbol{\theta}_e$ can converge to equilibrium point in finite time.

In order to attenuate the chattering phenomenon, for the terms $[\boldsymbol{s}^{2/3}]$ and $[\boldsymbol{s}^{1/3}]$ in eq. (10), $\mathrm{sign}(s_i)$ is replaced by $\mathrm{sat}(s_i)$ to design this control law, where

$$\mathrm{sat}(s_i) = \begin{cases} \tanh(s_i), | s_i | < \varepsilon_i, i = 1, \cdots, m \\ \mathrm{sign}(s_i), | s_i | \ge \varepsilon_i, i = 1, \cdots, m \end{cases} \tag{15}$$

In summary, the proposed controller can ensure the finite-time stability of the whole closed-loop system. The whole trajectory tracking process of the underwater manipulator is depicted in Fig. 2.

First, the desired joint positions of the manipulator end effector can be obtained by utilizing the desired trajectory via the inverse kinematics. And the FISMS (eq. (4)) is adopted and applied in the control scheme. The DO (eq. (8)) is introduced to estimate the lumped disturbances. Based on FISMC and DO, the second-order sliding-mode control law (eq. (10)) is used for the controller design. Then, a complete closed-loop system can be formed. Finally, the actual trajectory of the manipulator end effector can be acquired by the forward kinematics.

4. Simulation

Numerical simulations through MATLAB/Simulink Tool are performed on the 6 DOF underwater manipulator presented in section 2, in which its main link parameters are detailed in Table 1. Some other assumptions are given in this section about the system. Firstly, the density of its six hollow links for the manipulator is 2700kg/m^3. Assume that the positions of gravity centre and buoyancy centre are consistent; the density, velocity and acceleration of the fluid are 1025.9kg/m^3, [0.1, 0, 0] m/s and [0.01, 0, 0] m/s^2; the coefficient of water resistance is $C_D = 1.05$ and the coefficient of additional mass force is $C_M = 0.8$. Under these situations, it is still acknowledged that the target object moves in the workspace of the manipulator end effector, where its trajectory called the desired trajectory can be expressed as $(X_d, Y_d, Z_d) = (10\cos(\pi t/160) + 0.72,\ 10\sin(\pi t/160), 1)$ m for $\forall t \in [0, 300]$ s , and its orientation keeps coinciding with the base frame. The initial position of the manipulator

end effector is given by (10.72, 0, 1) m. The sample time of the simulation is 0.1s, and the number of the simulation steps N equals 3000. Simulations are operated under 5 different cases to validate the effectiveness of the control system, while the related parameters in the DO assigned as $\lambda_1 = 3$, $\lambda_2 = 1.5$, $\lambda_3 = 1.1$, $L = 0.1$ are suitable for all of those 5 cases.

Case 1-2: The external disturbances are only considered as the lumped disturbances, i.e. $\boldsymbol{d} = \boldsymbol{d}_\tau$, and the components of the vector are $d_{\tau 1} = 0.1\sin(0.15t) + 0.03\text{rad/s}^2$, $d_{\tau 2} = 0.1\cos(0.2t)\text{rad/s}^2$, $d_{\tau 3} = 0.1\sin(0.2t) + 0.01\text{rad/s}^2$, $d_{\tau 4} = 0.1\cos(0.2t)\,\text{rad/s}^2$, $d_{\tau 5} = 0.1\sin(0.15t) + 0.02\text{rad/s}^2$, $d_{\tau 6} = 0.1\cos(0.15t)\text{rad/s}^2$ for $t \in [50,150]\text{s}$, and in other time period, $\boldsymbol{d}_\tau = [0,0,0,0,0,0]^{\mathrm{T}}\,\text{rad/s}^2$. In this situation, the constant parameters of the proposed controller in eq. (10) are listed in Table 2. In case 2, the proposed controller with no DO method is utilized to handle the effects of the disturbances, while its other control parameters are the same with case 1.

Case 3-5: Consider this situation that the lumped disturbances contain both parameter uncertainties and the external disturbances, satisfying $\Delta\mathbf{M}(\boldsymbol{\theta}) = 0.1\mathbf{M}_0(\boldsymbol{\theta})$, $\Delta\mathbf{C}(\boldsymbol{\theta},\dot{\boldsymbol{\theta}}) = 0.1\mathbf{C}_0(\boldsymbol{\theta},\dot{\boldsymbol{\theta}})$, $\Delta\boldsymbol{G}(\boldsymbol{\theta}) = 0.1\boldsymbol{G}_0(\boldsymbol{\theta})$, $\Delta\boldsymbol{B}(\boldsymbol{\theta}) = 0.1\boldsymbol{B}_0(\boldsymbol{\theta})$, $\Delta\boldsymbol{\tau}_h = 0.1\boldsymbol{\tau}_{h0}$ and $d_{\tau 1} = 0.8\sin(0.15t)\text{rad/s}^2$, $d_{\tau 2} = 0.1\cos(0.2t)\text{rad/s}^2$, $d_{\tau 3} = 0.1\sin(0.2t)\text{rad/s}^2$, $d_{\tau 4} = 0.5\cos(0.2t)\,\text{rad/s}^2$, $d_{\tau 5} = 0.1\sin(0.2t)\text{rad/s}^2$, $d_{\tau 6} = \cos(0.15t)\text{rad/s}^2$ for $t \in [0,300]\text{s}$. In case 3, the control law of the DO-based PD control is designed as

$$\boldsymbol{U}_{PD} = -\mathbf{C}_2\boldsymbol{\omega}_e - \mathbf{C}_1\boldsymbol{\theta}_e - \hat{\boldsymbol{d}} - \boldsymbol{F}_\omega \tag{16}$$

For the DO-based PID-type linear SMC in case 4, its control law is

$$\boldsymbol{U}_{PID-SMC} = -\mathbf{C}_2\boldsymbol{\omega}_e - \mathbf{C}_1\boldsymbol{\theta}_e - \hat{\boldsymbol{d}} - \boldsymbol{F}_\omega - \sigma\cdot\text{sat}(\boldsymbol{s}) \tag{17}$$

with the PID-type linear sliding mode surface

$$\boldsymbol{s} = \boldsymbol{\omega}_e + \mathbf{C}_2\boldsymbol{\theta}_e + \mathbf{C}_1\int_0^t \boldsymbol{\theta}_e dt \tag{18}$$

Then, related constant parameters in case 3-5 are set to perform the following simulations and study the tracking performances of the system, where the parameters of the proposed controller in case 5 are selected referring to Table 2; the values of $\mathbf{C}_2$, $\mathbf{C}_1$ for both $\boldsymbol{U}_{PD}$ and $\boldsymbol{U}_{PID-SMC}$ are chosen the same as ones in case 5; to make the comparative fair, the terms σ and $\mathrm{sat}(\boldsymbol{s})$ in case 4 are valued at $\sigma = \max_{i=1,\cdots,6}(k_{wi}k_{pi})$ and same as in eq. (15), respectively.

Besides, for a clear comparison, the averaged position errors in three directions and their averaged total position error, and the averaged disturbance estimation error are defined as follows:

$$E_h = \sqrt{\| \boldsymbol{e}_h \|_2^2 / N},\ h = x, y, z, E_t = \sqrt{E_x^2 + E_y^2 + E_z^2}, E_d = \sqrt{\| \boldsymbol{e}_1 \|_2^2 / N} \tag{19}$$

where $\boldsymbol{e}_x, \boldsymbol{e}_y, \boldsymbol{e}_z$ indicate separately the X, Y, Z direction position error.

Only considering the external disturbances in case 1-2, some simulation results are shown in Figs. 3-10. In Fig. 3, the manipulator end effector has achieved the tracking control for the desired trajectory of the moving object. To further clarify the tracking results, Figs. 4- 6 describe the position errors between desired trajectory and tracking trajectory in X, Y and Z direction, respectively, under case 1 and case 2. From Figs. 4- 6, although all of the position errors in two cases may occur sudden changes at t=50s due to the external disturbances, finally their steady-state position errors can reach the range of about [-0.01, +0.01] m. Compared with case 1, the position errors in case 2 have caused a little larger chattering because the disturbances are not handled.

Figs. 7-8 describe the six components of the external disturbance term and their estimations in case 1, which show that their errors may have a little differences only at t=50s and t=150s. Such results are attributed to the DO which compensates the effect of the disturbances. Figs. 9-10 indicate the six joint input torques in case 1. It's obviously seen that the external disturbances have large influence on the joint input torques, especially at the periods of its sudden appearance and disappearance. Under such situations, the position errors and the disturbance estimation errors in case 1 can still keep in small regions, which can satisfy the requirements of the tracking performance. Seen from the averaged tracking errors in Table 3, although there are no significant differences of their averaged position errors between case 1 and case 2, the averaged disturbce estimation error in case 1 has a small value that shows the compensation for the effect of the external disturbances (see Figs. 7-8).

Subsequently, comparisons are made with PD control in case 3, PID-type linear SMC in case 4 and the proposed controller in case 5, where all of these methods need exploit the DO in Eq. 6 to deal with the lumped disturbance. Seen from Figs. 11- 13, three position errors in case 5 can obtain faster convergence than those in case 3 and case 4 at the beginning. Their three steady-state position errors can all reach the range of about [-0.01, +0.01] m in the final phase, while these steady-state errors in case 5 have much smoother changes than other two cases (see Figs. 11-13). Moreover, the averaged total position error in case 5 decreases about 0.003m compared to ones in both case 3 and case 4, shown in Table 3.

Figs. 14-15, Figs. 16-17 and Figs. 18-19 show six components of the lumped disturbance term and their estimations in case 3-5, respectively. It can be observed that, under the same DO method, the errors between the six disturbance components and

their estimations in case 3 are a little larger than those in case 4-5. This result can be obviously seen from their averaged disturbance estimation errors in Table 3, owing to the more superior SMC scheme than PD control.

In summary, simulation results under 5 different cases, show that the control system with the proposed scheme has better tracking performance and stronger robustness of disturbance rejection, which testifies the effectiveness of the proposed controller.

5. Conclusion

This paper proposes the FISMC strategy with a DO for the trajectory tracking control of the underwater manipulator under the lumped disturbances, including parameter uncertainties and external disturbances. The proposed FISMS is used so that the state error of the system can achieve the finite-time convergence. Meanwhile, the control scheme is designed by combining with the DO method and the second-order sliding mode control law, in which the DO is taken as a compensator to ensure that the estimation error can converge in finite time. In order to alleviate the chattering phenomenon, a saturated function is selected in the control law to replace the sign function. The closed-loop system is proved to be the finite-time stability by the stability analysis. Comparative simulation results show that the control system with the proposed scheme has better high-precision tracking performance and robustness of disturbance rejection, which demonstrates the feasibility and effectiveness of the proposed controller.

Appendix stability proof

Case 3: the DO-based PD control.

Taking eq. (16) into the error dynamics of system in eq. (6) instead of $\boldsymbol{U}_{\omega}$ results in

$$\dot{\boldsymbol{\omega}}_e + \mathbf{C}_2\boldsymbol{\omega}_e + \mathbf{C}_1\boldsymbol{\theta}_e = \boldsymbol{d} - \hat{\boldsymbol{d}} \tag{A1}$$

From the above analysis for the estimation error dynamics in eq. (9), we can acquire that the estimation error term $(\boldsymbol{d} - \hat{\boldsymbol{d}})$ is bounded, and after a finite time it can converge to zero. In view of the bounded-input bounded-output stable theory (Zheng and Chen 2018), the joint position error $\boldsymbol{\theta}_e$ can achieve the asympototic convergence to equilibrium point.

Case 4: the DO-based PID-type linear SMC.

Selecting another Lyapunov function

$$V_2 = 1/2\boldsymbol{s}^{\mathrm{T}} \cdot \boldsymbol{s} \tag{A2}$$

and taking its time derivative along eqs. (6), (17) and (18) yields

$$\begin{aligned} \dot{V}_2 &= \boldsymbol{s}^{\mathrm{T}}\dot{\boldsymbol{s}} \\ &= \boldsymbol{s}^{\mathrm{T}}(\dot{\boldsymbol{\omega}}_e + \mathbf{C}_2\boldsymbol{\omega}_e + \mathbf{C}_1\boldsymbol{\theta}_e) \\ &= \boldsymbol{s}^{\mathrm{T}}(\boldsymbol{F}_\omega + \boldsymbol{U}_{PID-SMC} + \boldsymbol{d} + \mathbf{C}_2\boldsymbol{\omega}_e + \mathbf{C}_1\boldsymbol{\theta}_e) \\ &= \boldsymbol{s}^{\mathrm{T}}(\boldsymbol{d} - \hat{\boldsymbol{d}}) - \sigma\boldsymbol{s}^{\mathrm{T}} \cdot \mathrm{sat}(\boldsymbol{s}) \\ &\le |\boldsymbol{s}|_1 \cdot |\boldsymbol{d} - \hat{\boldsymbol{d}}|_1 - \sigma\boldsymbol{s}^{\mathrm{T}} \cdot \mathrm{sat}(\boldsymbol{s}) \end{aligned} \tag{A3}$$

Similar to the discussion with eqs. (9) and (13), it can result from eq. (A3) that V_2 and s_i will be bounded in a finite time $[0, T_2]$. When the estimation error holds $e_1^i = 0$ for $t \ge T_2$, the derivative of the Lyapunov function satisfies $\dot{V}_2 = -\sigma\boldsymbol{s}^{\mathrm{T}} \cdot \mathrm{sat}(\boldsymbol{s}) \le 0$. Thus, the PID-type linear sliding mode surface s_i can achieve the asymptotic convergence to zero based on the Barbalat's Lemma. Then in the sliding mode phase $\boldsymbol{s} = \boldsymbol{0}$, by use of eq.

(18) it concludes that the joint position error θ_e can converge to equilibrium point asymptotically.

Declaration of conflicting interests

The author(s) declared no potential conflicts of interest with respect to the research, authorship, and/or pubilcation of this article.

Funding

This research has been supported by National Natural Science Foundation of China (No. 51979116), the HUST Interdisciplinary Innovation Team Project, the Innovation Foundation of Maritime Defense Technologies Innovation Center and the Fundamental Research Funds for the Central Universities, HUST: 2018JYCXJJ045, HUST: 2018KFYYXJJ012.

References

Antonelli, G. 2006. Underwater robots: motion and force control of vehicle-manipulator systems (Second Edition). Springer-Verlag Berlin Heidelberg.

Basin, M., Shtessel, Y., and Aldukali, F. 2016. Continuous finite- and fixed-time high-order regulators. J. Frankl. Inst. **353**(18): 5001-5012. doi:10.1016/j.jfranklin.2016.09.026.

Craig, J.J. 2005. Introduction to robotics mechanics and control (Third Edition). Pearson Education, Inc., Upper Saddle River, New Jersey.

Dinh, T.X., Thien, T.D., Anh, T.H., and Ahn, K.K. 2018. Disturbance observer based finite time tracking control for a 3 DOF hydraulic manipulator including actuator dynamics. IEEE Access, **6**: 36798-36809. doi:10.1109/ACCESS.2018.2848240.

Dunnigan, M.W., and Russell, G.T. 1998. Evaluation and reduction of the dynamic coupling between a manipulator and an underwater vehicle. IEEE J. Oceanic Eng. **23**(3): 260-273. doi:10.1109/48.701201.

Feng, Y., Han, F.L., and Yu, X.H. 2014. Chattering free full-order sliding-mode control. Automatica, **50**(4): 1310-1314. doi:10.1016/j.automatica.2014.01.004.

Huang, J., Ma, X., Che, H.C., and Han, Z.Z. 2019. Further Result on Interval Observer Design for Discrete-time Switched Systems and Application to Circuit Systems. IEEE Transactions on Circuits and Systems II: Express Briefs, **7747**(1): 1-1. doi: 10.1109/TCSII.2019.2957945.

Huang, J., Ma, X., Zhao, X., Che, H., and Chen, L. 2020. An interval observer design method for asynchronous switched systems, IET Control Theory Appl. doi:10.1049/iet-cta.2019.0750.

Hussian, A., Zhao, X.D., and Zong, G.D. 2017. Finite-time exact tracking control for a class of non-linear dynamical systems. IET Control Theory Appl. **11**(12): 2020-2027. doi:10.1049/iet-cta.2017.0093.

Lee, M., and Choi, H.S. 2000. A robust neural controller for underwater robot manipulators. IEEE Trans. Neural Netw. **11**(6): 1465-1470. doi: 10.1109/72.883478.

Liang, C.H., and Li, Y.C. 2014. Attitude tracking control based on adaptive sliding mode technique with double closed loop for spacecraft near small body. In Proceedings of the 17th International Conference on Computational Science and Engineering, Chengdu, China, 19-21 December 2014. pp. 78-82.

Liu, H.T., and Zhang, T. 2013. Neural network-based robust finite-time control for robotic manipulators considering actuator dynamics. Robot. Comput. Integr. Manuf. **29**(2): 301-308. doi:10.1016/j.rcim.2012.09.002.

Mobayen, S. 2015. An adaptive fast terminal sliding mode control combined with global sliding mode scheme for tracking control of uncertain nonlinear third-order systems. Nonlinear Dyn. **82** (1-2): 599-610. doi:10.1007/s11071-015-2180-4.

Pandian, S.R., and Sakagami, N. 2010. A neuro-fuzzy controller for underwater robot manipulators. In Proceedings of the 11th International Conference on Control Automation Robotics and Vision, Singapore, Singapore, 7-10 December 2010. pp. 2135-2140.

Patompak, P., and Nilkhamhang, I. 2012. Adaptive backstepping sliding-mode controller with bound estimation for underwater robotics vehicles. In Proceedings of the 9th International Conference on Electrical Engineering/Electronics, Computer, Telecommunications and Information Technology, Phetchaburi, Thailand, 16-18 May 2012. pp. 1-4.

Shtessel, Y.B., Shkolnikov, I.A., and Levant, A. 2007. Smooth second-order sliding modes: Missile guidance application. Automatica, **43**(8): 1470-1476. doi:10.1016/j.automatica.2007.01.008.

Sivcev, S., Coleman, J., Omerdic, E., Dooly, G., and Toal, D. 2018. Underwater manipulators: A review. Ocean Eng. **163**: 431-450. doi:10.1016/j.oceaneng.2018.06.018.

Wang, Y.Y., Gu, L.Y., Xu, Y.H., and Cao, X.X. 2016. Practical tracking control of robot manipulators with continuous fractional-order nonsingular terminal sliding mode. IEEE Trans. Ind. Electron. **63**(10): 6194-6204. doi:10.1109/TIE.2016.2569454.

Wang, Y.Y., Zhu, K.W., Chen, B., and Jin, M.L. 2019a. Model-free continuous nonsingular fast terminal sliding mode control for cable-driven manipulators. ISA Transactions, **98**: 483-495. doi:10.1016/j.isatra.2019.08.046.

Wang, Y.Y., Yan, F., Chen, J.W., Ju, F., and Chen B. 2019b. A new adaptive time-delay control scheme for cable-driven manipulators. IEEE Trans. Ind. Informat. **15**(6): 3469-3481. doi:10.1109/TII.2018.2876605.

Wang, Y.Y., Yan, F., Zhu, K.W., Chen, B., and Wu, H.T. 2019c. A new practical robust control of cable-driven manipulators using time-delay estimation. Int. J. Robust Nonlinear Control, **29**(11): 3405-3425. doi:10.1002/rnc.4566.

Wit, D.C.C., Diaz, E.O., and Perrier, M. 2000. Nonlinear control of an underwater vehicle/manipulator with composite dynamics. IEEE Trans. Control Syst. Technol. **8**(6): 948-960. doi:10.1109/87.880599.

Xu, G.H., Xiao, Z.H., Guo, Y., and Xiang, X.B. 2007. Trajectory tracking for underwater manipulator using sliding mode control. In Proceedings of the IEEE International Conference on Robotics and Biomimetics, Sanya, China, 15-18 December 2007. pp. 2127-2132.

Zheng, W.C., and Chen, M. 2018. Tracking control of manipulator based on high-order disturbance observer. IEEE Access, **6**: 26753-26764. doi:10.1109/ACCESS. 2018.2834978.

Table 1. The link parameters of the 6 DOF manipulator

Parameter	Link 1	Link 2	Link 3	Link 4	Link 5	Link 6
$\alpha_{i-1}(^\circ)$	0°	90°	0°	90°	-90°	-90°
$a_{i-1}(\mathrm{m})$	0	0	5.0	0	0	0
$d_i(\mathrm{m})$	1.195	0	0.7	6.4	-0.7	-0.995
$\theta_i(^\circ)$	θ_1	θ_2	θ_3	θ_4	θ_5	θ_6

Table 2. The parameters of the proposed controller

Case 1	Case 5
$\boldsymbol{\alpha}_2 = [7/8, 7/8, 7/8, 7/8, 7/8, 7/8]^{\mathrm{T}}$	$\boldsymbol{\alpha}_2 = [7/8, 7/8, 7/8, 7/8, 7/8, 7/8]^{\mathrm{T}}$
$\boldsymbol{\varpi}_2 = [9/8, 9/8, 9/8, 9/8, 9/8, 9/8]^{\mathrm{T}}$	$\boldsymbol{\varpi}_2 = [9/8, 9/8, 9/8, 9/8, 9/8, 9/8]^{\mathrm{T}}$
$\mathbf{C}_1 = \mathrm{diag}[4, 4, 4, 4, 4, 4]$	$\mathbf{C}_1 = \mathrm{diag}[4, 4, 4, 4, 4, 4]$
$\mathbf{C}_2 = \mathrm{diag}[4, 4, 4, 4, 4, 4]$	$\mathbf{C}_2 = \mathrm{diag}[4, 4, 4, 4, 4, 4]$
$\mathbf{K}_p = \mathrm{diag}[5, 5, 5, 5, 5, 5]$	$\mathbf{K}_p = \mathrm{diag}[10, 10, 10, 10, 10, 10]$

$\mathbf{K}_w = \mathrm{diag}[0.1, 0.1, 0.1, 0.1, 0.1, 0.1]$ $\mathbf{K}_w = diag[0.05, 0.05, 0.05, 0.05, 0.05, 0.05]$

$\boldsymbol{\varepsilon} = [0.3, 0.3, 0.3, 0.3, 0.3, 0.3]^{\mathrm{T}}$ $\boldsymbol{\varepsilon} = [0.3, 0.3, 0.3, 0.3, 0.3, 0.3]^{\mathrm{T}}$

Table 3. The averaged tracking errors of the system

Cases	E_x /m	E_y /m	E_z /m	E_t /m	E_d /N
Case 1	0.0123	0.0068	0.0236	0.0275	0.0079
Case 2	0.0124	0.0069	0.0237	0.0276	--
Case 3	0.0124	0.0141	0.0227	0.0295	0.5815
Case 4	0.0129	0.0102	0.0251	0.0300	0.0974
Case 5	0.0123	0.0069	0.0231	0.0270	0.0949

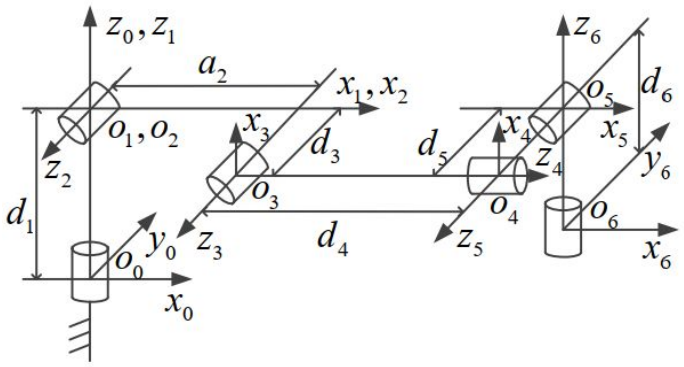

Fig. 1. The configuration of the 6 DOF manipulator and its link frames

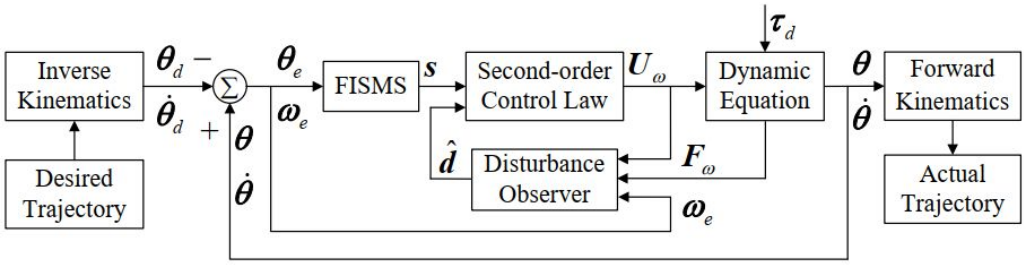

Fig. 2. The trajectory tracking control diagram

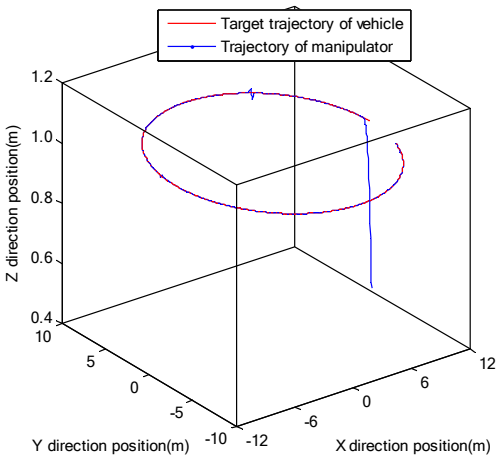

Fig. 3.The trajectories (case 1)

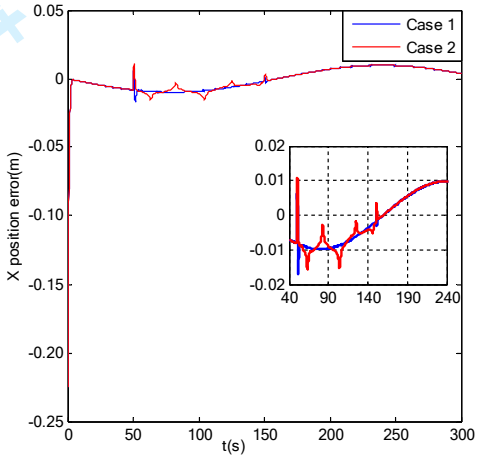

Fig. 4. X direction position error (case 1-2)

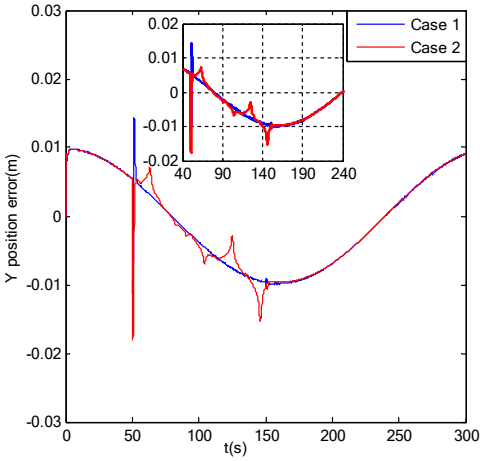

Fig. 5. Y direction position error (case 1-2)

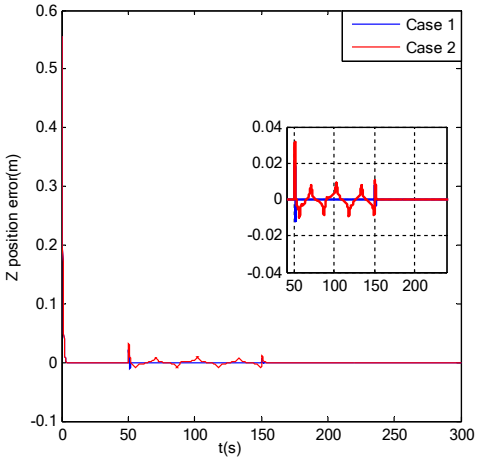

Fig. 6. Z direction position error (case 1-2)

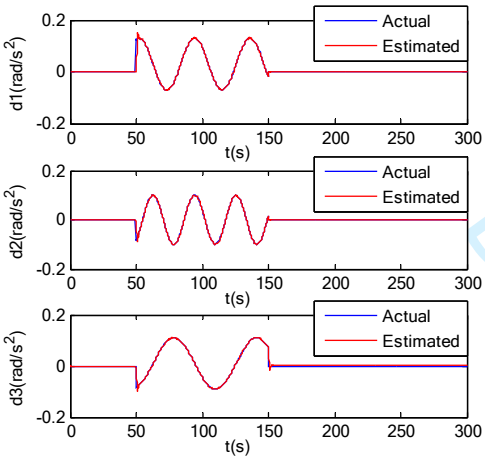

Fig. 7. d1-d3 and their estimates (case 1)

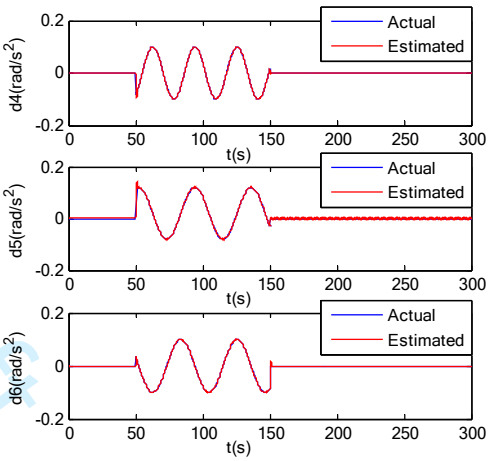

Fig. 8. d4-d6 and their estimates (case 1)

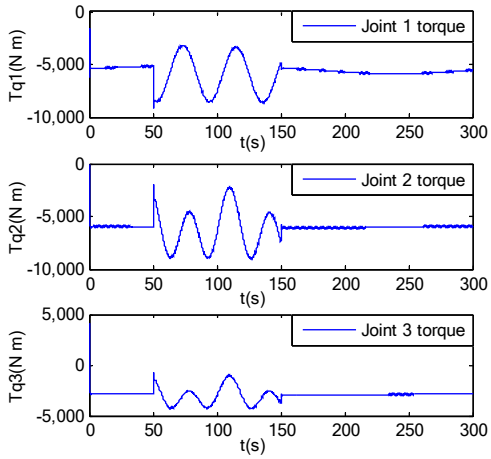

Fig. 9. Joint 1-3 input torques (case1)

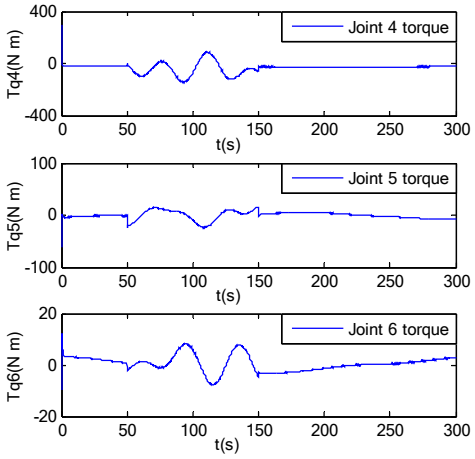

Fig. 10. Joint 4-6 input torques (case 1)

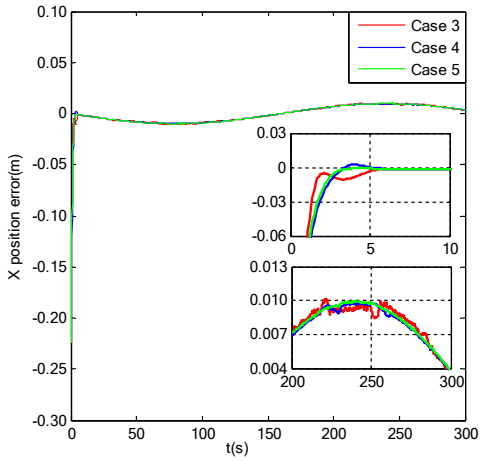

Fig. 11. X position error (case 3-4-5)

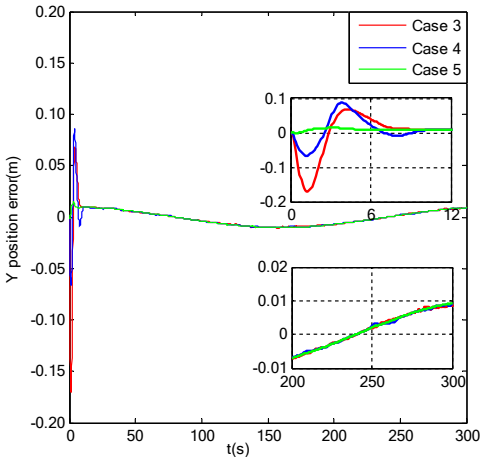

Fig. 12. Y position error(case 3-4-5)

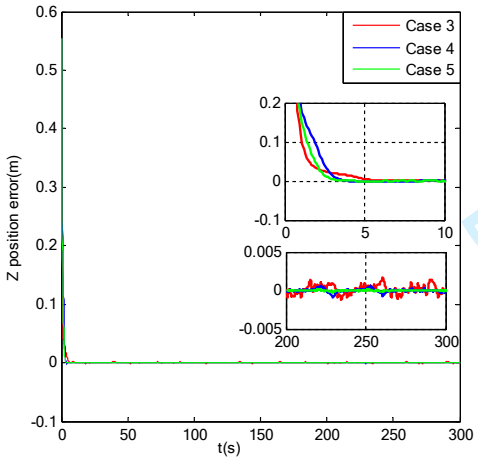

Fig. 13. Z position error(case 3-4-5)

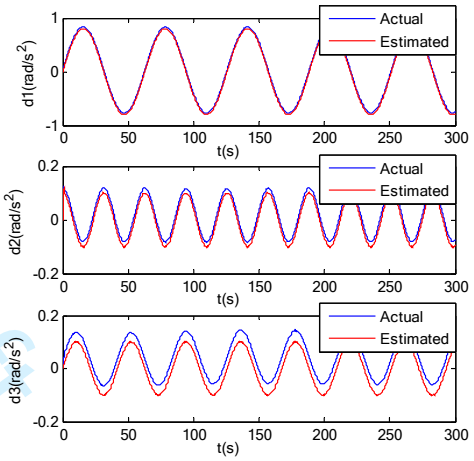

Fig. 14. d1-d3 and their estimates (case 3)

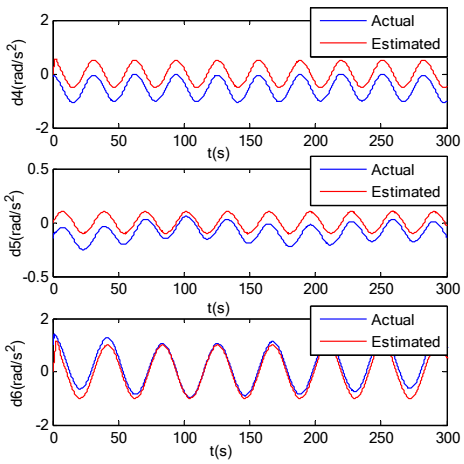

Fig. 15. d4-d6 and their estimates (case 3)

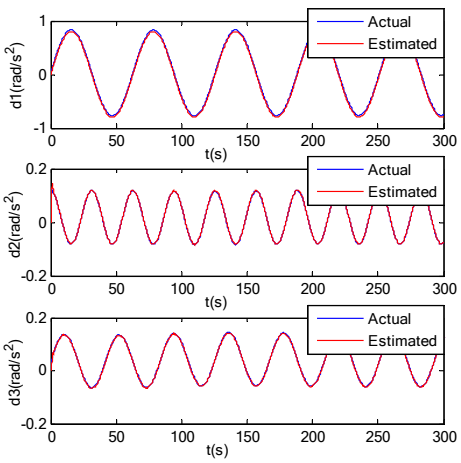

Fig. 16. d1-d3 and their estimates (case 4)

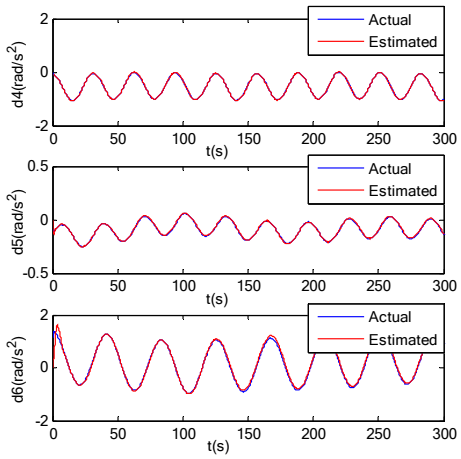

Fig. 17. d4-d6 and their estimates (case 4)

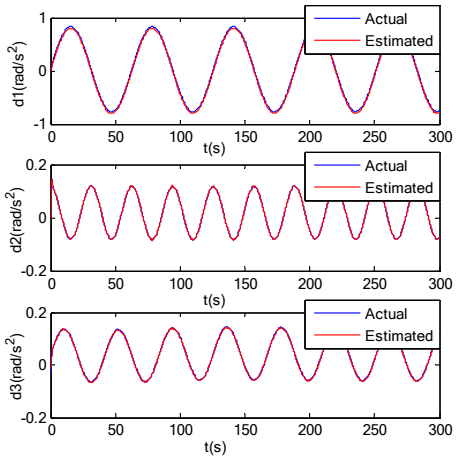

Fig. 18. d1-d3 and their estimates (case 5)

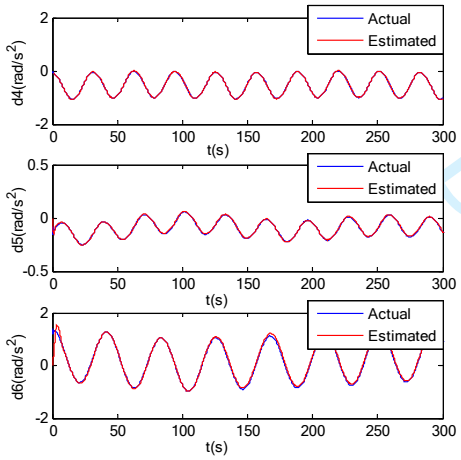

Fig. 19. d4-d6 and their estimates (case 5)